

Formation of Rydberg States in Fast Ions Penetrating Thin Carbon-Foil and Gas Targets

G. Schiwietz, D. Schneider, and J. Tanis^(a)

Bereich Kern- und Strahlenphysik, Hahn-Meitner-Institut für Kernforschung, 1000 Berlin 39, Germany

(Received 25 June 1987)

The absolute field-ionization yields of gas- and foil-excited Rydberg states are measured for different fast beam ions. From the yields a direct comparison of the quantum-state populations of high- n states ($n > 100$) produced by gas and foil excitation could be obtained. Model calculations are consistent with the high- n states being predominantly produced by excitation of the projectile or capture of target electrons in the last layers of the solid target.

PACS numbers: 34.50.Fa, 34.60.+z, 34.70.+e

Near-threshold excitation, where electron capture into projectile-centered continuum or Rydberg states occurs in interactions of fast highly charged projectiles with solids, has been intensively investigated for some time.¹ Yet there is still no sufficient theoretical model to account for the various experimental findings. Studies concerned with the formation of Rydberg states (highly excited hydrogenlike states with large n quantum numbers) in fast ions emerging from foil targets help to provide an understanding of the processes involved in the threshold excitation in ion-solid interactions.²

Since Rydberg states have considerably larger electronic orbitals than the lattice spacings in a solid, it is assumed that the Rydberg states are formed by collisional interactions in the last layers of the penetrated solid. One of the major questions addressed in this research is the effect of various bulk and surface processes in the ion-solid interaction on the population of Rydberg states, the angular distribution of convoy electrons, and their mean free path. Burgdörfer and co-workers³ have developed a classical transport theory for electrons near threshold under the influence of stochastic scattering processes in the solid and a strong ionic Coulomb field. This approach may illuminate the problem of the stability of Rydberg orbits under the influence of stochastic perturbations as well as the transmission of convoy electrons through solids.

Recently reported results, where the delayed Lyman- α and $-\beta$ radiation has been measured from fast ($v \approx 10$ a.u.) foil-excited ions, suggested that the Rydberg-state production accentuates high- l states and is more than 2 orders of magnitude larger than could be explained by last-layer electron capture.⁴ Measurements of the light emission from foil-excited Rydberg states near the yrast line in fast F- and Si-beam ions have also been reported recently.² In both cases, the data were described quite well with an empirical parametrization for the average population per nl Rydberg state, with the light emission showing a dependence on the core charge of the penetrating ions as well as on the nuclear charge. This is consistent with a picture where electron capture dominates the production of Rydberg states. The Rydberg-state population of a certain final charge state seems to

be almost strictly proportional to the corresponding population of a given core-charge-state fraction. It is, however, not possible to distinguish between capture of target electrons and recapture of cusp electrons or successive capture and excitation processes.

Measurements of the absolute yield of beam-foil-excited Rydberg states have been reported previously for the case of 125-MeV S¹⁴⁺ ions excited in thin carbon foils.⁵⁻⁷ The absolute yields of the Rydberg states were measured with the use of field-ionization techniques. The measured yields compared well with estimates of the quantum-state population for high- n states ($n = 250$ to 650) based on a theoretical cross-section value for capture of carbon $1s$ electrons into Rydberg states (given in Ref. 4) and the mean free path for collisional depopulation of these high- n states, which was set equal to the mean free path for free-electron scattering.⁸ This result was consistent with the assumption of last-layer capture (\approx eight layers) being responsible for the formation of the high- n states. It is, however, in disagreement with the indirectly determined results of Rothermel *et al.*⁴ for 127-MeV S¹⁶⁺ + C. The present experiments give, for the first time, a direct comparison between the probabilities for Rydberg-state population ($n \geq 100$) following foil and gas excitation of fast ions.

The measurements were conducted at the VICKSI heavy-ion facility at the Hahn-Meitner-Institut, Berlin. The experimental setup is similar to the one described in detail by Schneider *et al.*⁹ A tightly collimated beam of ions traverses a carbon-foil or gas target. The thickness of the carbon foil is 20 $\mu\text{g}/\text{cm}^2$; the gas cell is 10 cm long and the gas pressure in the cell is maintained at 38 mTorr to ensure single-collision conditions with respect to charge transfer and excitation. After having traveled a distance of 7 cm from the gas-target-cell exit or 17 cm from the foil target, the ion beam traverses the first stage of an electrostatic 45° parallel-plate tandem electron spectrometer. The electric field of the first stage of the spectrometer serves to extract electrons from projectile Rydberg states by field ionization and to separate the extracted electrons from the beam. The electrons are analyzed and are finally recorded by means of an electron multiplier.

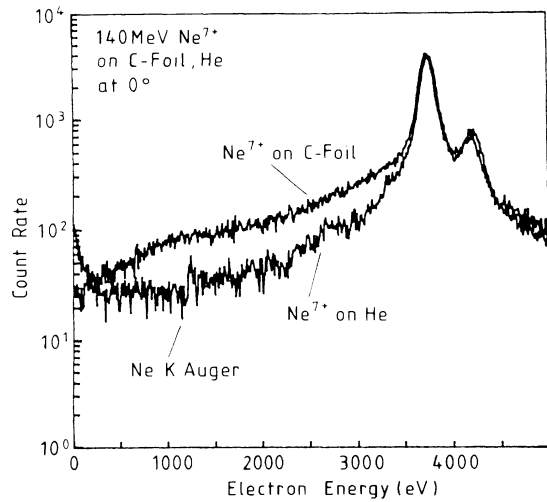


FIG. 1. Total electron spectra following the excitation of 140-MeV Ne^{7+} ions in a $20\text{-}\mu\text{g}/\text{cm}^2$ C foil and a He-gas target.

Typical electron spectra following 140-MeV Ne^{7+} gas and foil excitation are shown in Fig. 1. The spectra are dominated by the cusp peak centered at an energy which corresponds to electrons traveling with the beam velocity. Depending on the excitation process, these electrons stem from electron capture to the continuum, electron loss to continuum, or convoy electrons (solid target). The smaller peak at slightly higher energy is due to Rydberg-state electrons. The spectrometer entrance slit causes a fringe field, so that electrons resulting from field ionization of projectile Rydberg states in the first stage of the spectrometer are observed at an "apparent" energy somewhat larger than the cusp energy since field ionization takes place only after the Rydberg ions have traveled a short distance into the spectrometer, thereby requiring a higher analyzer energy for detection. The yields for electrons contributing to field-ionized Rydberg states are determined from the integrated counting rate after back-

ground subtraction. The two structures ("cusp" and Rydberg peak) are well separated in the spectrum.

The electrons from atoms which are ionized in the spectrometer field are detected in an open electron multiplier after passing the second stage of the analyzer. The efficiency of the detector system was confirmed by auxiliary measurements where Ar-L Auger electrons have been measured at 0° following collisions of 200-keV H^+ on Ar. The known cross section for the Ar-L Auger-electron production¹⁰ was used to determine the efficiency of the electron spectrometer. The transmission T of field-extracted Rydberg electrons through the spectrometer was about 7×10^{-3} . The absolute Rydberg yields for the different cases where foils and gases have been used for excitation are given in Table I; also shown are the mean core charges of ions, the ionizing field in the spectrometer required to analyze beam-velocity electrons, and the corresponding minimum quantum number of extracted Rydberg electrons n_{\min} (classical estimate). An upper limit n_{\max} for the field-ionized Rydberg states corresponds to the contact potentials. This upper limit has only a small effect on the absolute Rydberg yields. The absolute Rydberg yield per incident ion is

$$Y_R = \sum_i N_i (\Delta E_i / \epsilon E_i T) (\bar{q}e / Q), \quad (1)$$

and, under the assumption of a production mechanism (capture or excitation) that produces a Rydberg-state population $P(n)$ which varies as $P_0 n^{-3}$ (Ref. 4), the yield can be expressed as

$$Y_R = 0.5 P_0 [n_{\min}^{-2} - n_{\max}^{-2}]. \quad (2)$$

Here P_0 is a constant giving the strength of the Rydberg-state population, N_i is the number of counts obtained after background subtraction when the spectrometer is set to analyze electrons of energy E_i , and ΔE_i is the change in analyzed energy for each step. The relative energy resolution of the spectrometer was $\epsilon = \delta E_i / E_i = 0.036$ (full width at half maximum). The total charge collected in the Faraday cup is Q and $\bar{q}e$ is the mean charge of the emerging ions.

TABLE I. Absolute field-ionization yields Y_R and quantum-state populations $P(n)$; also given are the projectiles, their energies, mean charge states of the outgoing projectile \bar{q} , and the ionizing field F_s (V/cm) in the spectrometer. The theoretical Rydberg state populations were derived from the predicted excitation, capture and electron-loss cross sections using Eq. (3).

Projectile	Target	\bar{q}	Experiment				Theory			
			F_s (V/cm)	$10^5 Y_R$ per ion	n_{\min}^a	$P(n)n^3$	$n^3 \sigma_E$ (10^{-20} cm^2)	$n^3 \sigma_C$ (10^{-20} cm^2)	σ_L (10^{-20} cm^2)	$P(n)n^3$
139-MeV Ne^{7+}	Foil ^b	9.5	2159	0.516	136	0.19	87×0.5^c	39	316	0.25
	He gas	7		0.38	108	0.089				
125-MeV $\text{S}^{14+ d}$	Foil	15	860	1.7	240	2.1	39	1040	559	1.82
	He gas	23	1207	25.6	314	50	2140	9240	569	18.9
226-MeV Ni^{10+}	He gas	10		2.32	170	1.34	10200		128	1.27
	Foil	27	939	34.2	363	90	2460	44700	724	63
He gas	14	6.48		223	6.4	11700		164	1.45	

^a $F_s = 10^9 \bar{q}^3 / n_{\min}^4$ V/cm.

^bFoils are $20 \mu\text{g}/\text{cm}^2$.

^cMeasured with a single-stage spectrometer.

^dCross section multiplied with 9^+ charge-state fraction.

The following discussion shows that it is possible to explain measured Rydberg-electron yields within a simple multiple-collision picture. Rydberg states are populated either by capture of target electrons or by collisional excitation of the projectile, determined, respectively, by capture and excitation cross sections σ_C and σ_E . The depopulation of Rydberg states is determined by the cross section for direct ionization σ_L . With the assumption that the projectile core charge state equilibrates rapidly inside the foil, the population of a Rydberg state with principal quantum number n can be derived from rate equations (for a detailed discussion see the review of Betz¹¹) as follows:

$$P(n) = \sum_q f(q) \{[\sigma_C(n,q) + \sigma_E(n,q)]/\sigma_L\} [1 - \exp(-\sigma_L d)]. \quad (3)$$

The charge-state fractions are denoted by $f(q)$, and d is the number of target atoms per square centimeter. To simplify the evaluation of Eq. (3) we performed the cross-section calculations only for the mean exit charge state in each case. The capture cross sections in Table I were extracted from classical-trajectory Monte Carlo calculations in the independent-particle model¹² for final main quantum numbers from $n=1$ to 8. It was found that the cross sections scale as n^{-3} (as in the case of the Oppenheimer-Brinkman-Kramers or the Jackson-Schiff approximation^{13,14}) for $n \geq 5$. Strong deviations (up to a factor of 100) from this dependence were found for lower n values, however.

The electron-loss cross-section calculations were performed in the plane-wave Born approximation (PWBA) according to the prescription of Bates and Griffing.¹⁵ A projectile-electron-target interaction potential

$$V(\mathbf{R}, \mathbf{r}) = - \left[Z_{\text{eff}} + \frac{Z_T}{|\mathbf{R} - \mathbf{r}|} \right] \exp(-2Z_{\text{eff}}|\mathbf{R} - \mathbf{r}|) \quad (4)$$

was chosen, which is exact for an atomic-hydrogen target if the target electron remains in the ground state during the collision. For the present cases we chose an effective charge $Z_{\text{eff}}=1.68$ for the helium target (Hartree-Fock result) and $Z_{\text{eff}}=2.05$ for the carbon target [taken from the Thomas-Fermi model, $Z_{\text{eff}}=(Z_T/0.885)^{1/3}$]. Since hydrogenlike projectile wave functions scale like Z_p/n near the nucleus, we used

$$\sigma_L(1s \rightarrow \epsilon, Z_p/n) \approx \sigma_L(n \rightarrow \epsilon, Z_p) \quad (5)$$

to estimate the electron-loss cross sections as investigated in detail by Röschenhaler *et al.*¹⁶

The excitation cross sections were also estimated in the PWBA with use of the form factors by Cheshire and Kyle¹⁷ and the scaling mentioned above for electron loss. For most of the cases the initial as well as the final states were approximated by the Z_p/n scaling. Therefore we compared these results with PWBA ionization cross sections (using correct Coulomb continuum wave functions) $d\sigma/dE$ ($E=0$) multiplied by Z_p^2/n^3 to compute excitation cross sections. Both methods should yield similar results if $(d\sigma/dE)(E \leq 0) \approx (d\sigma/dE)(E \geq 0)$. From the deviations between these separate calculations it was estimated that the listed values have uncertainties of a factor 3 in the framework of the PWBA. It should be

mentioned that the use of projectile Coulomb wave functions may result in additional uncertainties, since the investigated Rydberg states should be strongly influenced by the (screened) wake potential inside the solid.¹⁸

From Table I it is observed that the yields Y_R of electrons from the field ionization of high- n states are comparable for the cases of gas and foil excitation. This is significant since the yields following gas excitation were measured under single-collision conditions. An error of about 50% must be taken into account for the absolute field-ionization yields and is mainly due to the uncertainty of the transmission of the tandem spectrometer and to coherence effects.⁹ Furthermore, Table I shows very good agreement between the theoretical and experimental $P(n)n^3$ quantum-state populations for the gas as well as for the foil case. Within the experimental error, the ratios of the $P(n)n^3$ between foil and gas excitation are found to increase with increasing projectile Z .

The excellent agreement between theoretical and experimental quantum-state population numbers indicates that last-layer (meaning the last 50 layers or so) electron capture is responsible for populating near-threshold states in ion-solid interactions. These results also suggest that Rydberg states seem to survive more collisions in the solid than free electrons would and, additionally, that higher-order solid effects are negligible. Since in ion-solid collisions Rydberg electrons undergo multiple collisions and are also influenced by a nonspherical wake potential (which may result in a Stark mixing of different substates¹⁹) we expect the orbital angular momentum states to be nearly statistically populated.

We would like to thank U. Stettner, T. Schneider, H. Platten, N. Stolterfoht, and Y. Yamazaki for experimental support and helpful discussions.

(a)On leave from Western Michigan University, Kalamazoo, MI 49008.

¹M. Breinig, S. B. Elston, S. Huldt, L. Liljeby, C. R. Vane, S. D. Berry, G. A. Glass, M. Schauer, I. A. Sellin, G. D. Alton, S. Datz, S. Overbury, R. Laubert, and M. Suter, *Phys. Rev. A* **25**, 3015 (1982).

²K. Dybdahl, J. Sørensen, P. Hvelplund, and H. Knudsen, *Nucl. Instrum. Methods Phys. Res., Sect. B* **13**, 581 (1986).

³J. Burgdörfer and C. Botcher, *Abstracts of Contributed*

Papers, Proceedings of the Fifteenth Conference on the Physics of Electronic and Atomic Collisions, Brighton, England, 1987, edited by J. Geddes *et al.* (to be published).

⁴H.-D. Betz, D. Rösenthaller, and J. Rothermel, Phys. Rev. Lett. **50**, 34 (1983); J. Rothermel, H.-D. Betz, F. Bell, and V. Zacek, Nucl. Instrum. Methods **194**, 341 (1982).

⁵E. P. Kanter, D. Schneider, and Z. Vager, Phys. Rev. A **28**, 1193 (1983).

⁶E. P. Kanter, D. Schneider, Z. Vager, D. S. Gemmell, B. J. Zabransky, Gu Yuan Zhuang, P. Arcuni, P. M. Koch, D. R. Mariani, and W. Van de Water, Phys. Rev. A **29**, 583 (1984).

⁷Z. Vager, B. J. Zabransky, D. Schneider, E. P. Kanter, Gu Yuan Zhuang, and D. S. Gemmell, Phys. Rev. Lett. **48**, 592 (1982).

⁸P. M. Koch, Phys. Rev. Lett. **43**, 432 (1979); M. P. Seah and W. A. Dench, Surf. Interface Anal. **1**, 2 (1979).

⁹D. Schneider, W. Zeitz, R. Kowallik, G. Schiwietz, T. Schneider, N. Stolterfoht, and U. Wille, Phys. Rev. A **34**,

169 (1986).

¹⁰N. Stolterfoht, D. Schneider, and P. Ziem, Phys. Rev. A **10**, 81 (1974).

¹¹H.-D. Betz, Rev. Mod. Phys. **44**, 465 (1972).

¹²G. Schiwietz and W. Fritsch, J. Phys. B (to be published).

¹³K. Omidvar, Phys. Rev. A **12**, 911 (1975); F. T. Chan and J. Eichler, Phys. Rev. A **20**, 1841 (1979).

¹⁴J. D. Jackson and H. Schiff, Phys. Rev. **89**, 359 (1953).

¹⁵D. R. Bates and G. Griffing, Proc. Phys. Soc. London, Sect. A **66**, 961 (1953).

¹⁶D. Rösenthaller, H.-D. Betz, J. Rothermel, and D. H. Jakubassa-Amundsen, J. Phys. B **16**, L233 (1983).

¹⁷I. M. Cheshire and H. L. Kyle, Phys. Lett. **17**, 115 (1965).

¹⁸P. M. Echenique, R. H. Ritchie, and W. Brandt, Phys. Rev. B **20**, 2567 (1979).

¹⁹J. P. Rozet, A. Chetioui, P. Bouisset, D. Vernhet, K. Wohrer, A. Touati, C. Stephan, and J. P. Grandin, Phys. Rev. Lett. **58**, 337 (1987).